Noninvasive neuroelectronic interfacing with synaptically connected snail neurons immobilized on a semiconductor chip

Günther Zeck and Peter Fromherz*

Department of Membrane and Neurophysics, Max Planck Institute for Biochemistry, D 82152 Martinsried/Munich, Germany

A hybrid circuit of a semiconductor chip and synaptically connected neurons was implemented and characterized. Individual nerve cells from the snail *Lymnaea stagnalis* were immobilized on a silicon chip by microscopic picket fences of polyimide. The cells formed a network with electrical synapses after outgrowth in brain conditioned medium. Pairs of neurons were electronically interfaced for noninvasive stimulation and recording. Voltage pulses were applied to a capacitive stimulator on the chip to excite the attached neuron. Signals were transmitted in the neuronal net and elicited an action potential in a second neuron. The postsynaptic excitation modulated the current of a transistor on the chip. The implementation of the silicon-neuron-neuron-silicon circuit constitutes a proof-of-principle experiment for the development of neuroelectronic systems to be used in studies on neuronal signal processing, neurocomputation, and neuroprosthetics.

The combination of microelectronics and of circuits with nerve cells has a touch of science fiction with an outlook on brain chips and neurocomputers. At present two approaches may be distinguished: (*i*) Networks of nerve cells have been emulated by microelectronic circuits in silicon to improve signal processing of conventional circuitry (1). (*ii*) Electronic circuits have been joined to nerve cell circuits via impaled micropipettes to supplement and investigate biological function (2). If, however, nerve cell circuits and electronic devices could be interweaved at a microscopic level, we could integrate them in a far more sophisticated manner: a nerve cell circuit could support electronic data processing even if the underlying mechanisms are unknown, and complete electronic control of a network of nerve cells could help unravel the nature of biological neurodynamics. One goal would be the assembly of a neuronal net with associative memory (3) that is supervised by a semiconductor substrate (Fig. 1*A*). Long-term studies of such hybrid circuits require a noninvasive electronic interface without electrochemical reactions at the substrate.

In the present paper, we demonstrate the feasibility of neuroelectronic systems in a proof-of-principle experiment. We implement the elementary unit of such systems, the signaling from a chip through a monosynaptic neuronal loop back to the chip (Fig. 1*B*). We do not pursue array-recording of neuronal systems (4–6), but rather a controlled interfacing of a minimal nerve cell circuit by a semiconductor device, continuing studies on capacitive stimulation, transistor recording, and two-way interfacing of individual neurons (7–10). Silicon without exposed metal is our substrate of choice because insulating the chip with a thin layer of silicon dioxide avoids electrochemical processes at the electronic–biological interface. The silica film also forms an inert and homogeneous surface for cell culture. Another obvious advantage of silicon is that local electronic devices can be integrated by standard semiconductor technology (11). In our approach, invertebrate nerve cells are preferred because their large cell bodies support efficient interfacing and because small networks have a biological function and can be reconstituted in cell culture (12–14). In the present study, we used neurons from the pedal ganglia of *Lymnaea stagnalis* (15,

16), which interconnect in culture via strong electrical synapses (17–19).

A two-way contact on a silicon chip for electronic interfacing of a nerve cell consists of a stimulator and a transistor (9). The stimulator is a p-doped area in n-silicon covered by a thin layer of silicon dioxide. It is suitable for capacitive signal transfer from the chip to a nerve cell (8). The field-effect transistor consists of p-doped regions of source and drain with a gate area covered by a thin oxide without metal. It probes the extracellular voltage beneath an attached nerve cell (7). The electrical features of an electronically interfaced monosynaptic loop are described by the equivalent circuit of Fig. 1*C*, with the intracellular voltages V_M and the extracellular voltages V_J in the junctions. In a previous attempt to implement neuron-silicon circuits, it was found that the cell bodies of snail neurons were displaced from their primary contact sites on a chip by the forces exerted by outgrowing neurites (19). That structural instability prevented a reproducible formation of silicon-neuron-neuron-silicon circuits. Here, we solved that problem by mechanical fixation, using open picket fences on the chip to immobilize the cell bodies on their two-way contacts.

Materials and Methods

Chip. We used 100 n-type silicon wafers (diameter 100 mm, resistance 2–4 Ω·cm). Two-way contacts were fabricated where each transistor was surrounded by two wings of a stimulator (10, 19). Sixteen contacts were arranged on a circle such that attached neurons could interact in a central area with their outgrowing neurites. Chip preparation followed previous protocols (10, 19, 20). First, the lateral insulation of the transistors and stimulators was made by local oxidation of silicon. Then the transistor leads and the stimulators were doped by boron implantation. A passivation oxide (600 nm) was deposited by plasma-enhanced chemical vapor deposition and removed with fluoric acid in the central area of the chip where the two-way junctions are located. Then a thin oxide (10 nm) was grown on the central area, which covered stimulators and transistors. The leads of the transistors were joined to the gate area by boron implantation. Length and width of the p-channel were 2 μm and 8 μm. We bonded the chip to a standard ceramic package (Spectrum CPGA 208L, San Jose, CA) and attached a circular chamber of perspex (bottom diameter 4 mm) by using a medical glue (MK3, Sulzer Osypka, Grenzach Wyhlen, Germany).

Picket Fences. We fabricated fences of vertical pickets from polyimide in a photolithographic process that did not interfere with the electronic function of the chip (21). After dehydrating the chip at 200°C for 2 h, a photosensitive polyimide (HTR3-200,
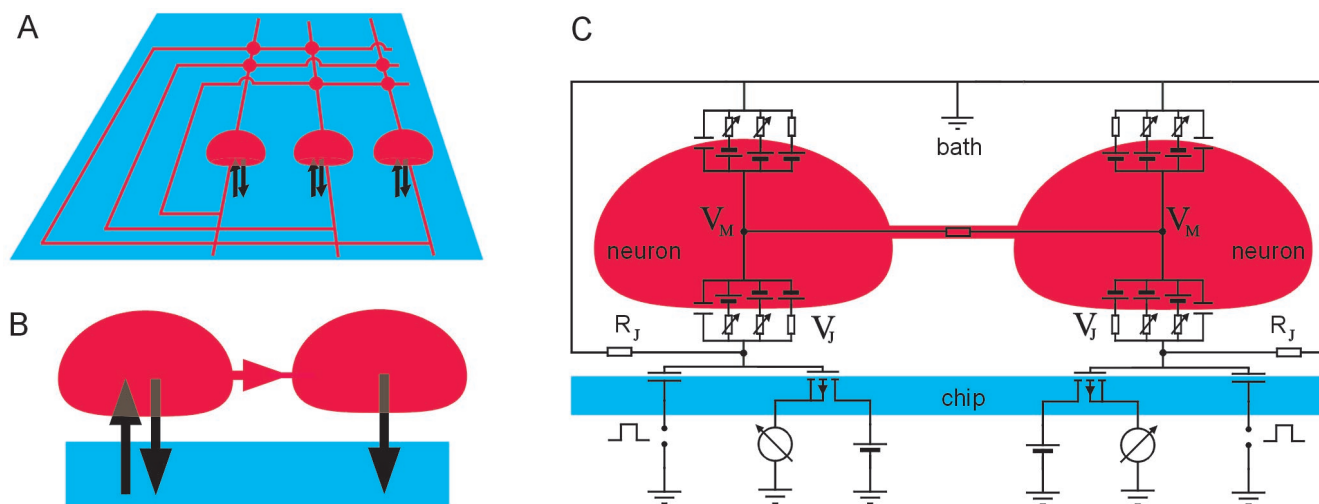

NEUROBIOLOGY

Fig. 1. Neuroelectronic systems. (*A*) Network of nerve cells (red) with controlled connections of axons, synapses, and dendrites supervised from a semiconductor chip (blue) by two-way interfacing (black). (*B*) Elementary silicon-neuron-neuron-silicon circuit with presynaptic stimulation and recording, synaptic transmission, and postsynaptic recording. (*C*) Equivalent circuit of neuron pair connected by an electrical synapse and interfaced by capacitive stimulators and field effect transistors. The cells are separated from the chip by a narrow gap filled with electrolyte (not on scale, width of the gap 50 nm, diameter 50 μm). The junctions are described by a global resistance R_J; the free and attached cell membranes by capacitances, Ohmic and voltage-dependent conductances; and the synapse by an Ohmic conductance. V_M are intracellular voltages; V_J are extracellular voltages in the junctions. Voltage pulses at the stimulator excite a neuron by capacitive coupling through the gap. A firing neuron gives rise to an extracellular voltage in the gap that modulates the source-drain current of the transistor.

OCG, Munich, Germany) was spin coated at 700 rpm for 20 s. We prebaked the chip for 4 h—starting at 40°C and ending at 80°C—and illuminated it for 1.5 min in near UV-light through a mask. The shielded polyimide was removed by using a spray-development technique. The fences were cured at 300°C for 3 h under nitrogen. The pickets had a height of 40 μm and a diameter of 25 μm.

Neurons. Pond snails *L. stagnalis* were raised in tap water and fed on lettuce. The preparation of neurons followed previous protocols (15, 16, 18). Snails were deshelled, soaked in 25% lysterine in normal saline consisting of (in mM) NaCl 51.3, KCl 1.7, CaCl$_2$ 4.1, MgCl$_2$ 1.5, and Hepes 5.0 at pH 7.9 (all from Sigma), and fixed to a Sylgard (Sylgard 184, Dow Corning, Midland, MI) dish containing antibiotic saline (with 150 μg/ml gentamycin). Central ganglion rings were dissected, soaked in antibiotic saline three times for 10 min, and pinned on a small Sylgard dish. After removing the outer sheath, the brains were treated with 1.33 mg/ml collagenase/dispase (Boehringer Mannheim) and 0.67 mg/ml trypsin (Sigma, T8253) for 30 min in defined medium, washed several times, treated with 0.67 mg/ml trypsin inhibitor (Sigma, T9003) in defined medium for 15 min, and washed again. Then high-osmolarity medium (defined medium with 30 mM glucose) was applied. The pedal ganglia were opened with a tungsten microneedle. Neurons from the A-clusters were removed by suction through a fire-polished, silanized micropipette.

Cell Culture. The chips were cleaned by local application of freshly prepared piranha solution (30% hydrogen peroxide, 96% sulfuric acid, volume ratio 1:2) and extensively rinsed with milli-Q water. After sterilization in UV-light (30 min), they were coated with poly-L-lysine (P6516, Sigma) by adsorption from a 1 mg/ml solution in 0.15 M Tris·HCl buffer at pH 8.4 for 4 h and rinsed again. Cell culturing followed previous protocols (16, 19, 22, 23). The chamber was filled with 600 μl of defined medium (PAN Systems, Aidenbach, Germany) with (in mM) NaCl 40.0, KCl 1.7, CaCl$_2$ 4.1, MgCl$_2$ 1.5, glutamine 1.0, Hepes 10.0 (pH 7.9), and all other ingredients of Leibovitz L15 medium at half of the standard concentrations, with 20 μg/ml gentamycin (Sigma, G3632). Individual neuronal cell bodies were placed into the

picket fences by using a glass micropipette. Two complete brains were placed onto a terrace of the chamber to condition the medium and to promote outgrowth. The neurons were incubated at 20°C for two to three days.

Gap Width. We measured the distance between the cell membrane and the chip by fluorescence interference contrast (FLIC) microscopy (24, 25). The neurons were grown on special silicon chips with microscopic terraces of silicon dioxide (area 5 μm × 5 μm, four heights from 10 nm to 140 nm) under the same conditions as described above. We added 30 μl of a 2 mM ethanolic solution of the amphiphilic cyanine dye DiIC$_{18}$ (Molecular Probes) to the culture medium and replaced the staining solution by fresh medium after 15 min. Fluorescence micrographs were taken through a water immersion objective (×63, numerical aperture 0.9, Zeiss Axioskop) with an illumination at 546 nm and a detection at 580–640 nm using a charge-coupled device (CCD) camera. On each terrace, we observed a rather homogeneous fluorescence of the attached cell membrane. From a fit of the four intensities by the electromagnetic FLIC theory, we obtained the width d_J of the gap between membrane and chip.

Gap Resistance. The sheet resistance of the gap between neuron and chip was obtained from the response of a membrane-bound voltage-sensitive dye to electrical stimulation from the chip (26). The cells were cultured on a special silicon chip with a thin homogeneous silicon dioxide (15 nm) and with electrical contacts on the back by using the same conditions as described above. The cell membrane was stained with the amphiphilic hemicyanine dye 8-*N*,*N*-dibutylamino-2-azachrysene-butylsulfonate (Annine 5) by adding 10 μl of a 3 mM dye/HCl solution to the culture medium and replacing the solution by fresh medium after 5 min (G. Hübener, B. Kuhn, and P.F., unpublished results). Fluorescence pictures were taken with a confocal microscope (FluoView, Olympus, New Hyde Park, NY) at an illumination of 472.7 nm (Ar laser, Spectra-Physics) and a detection between 540–680 nm (26). An AC voltage (amplitude 1 V, frequency 2 kHz) was applied between chip and bath, and the relative change of fluorescence in the attached region of the
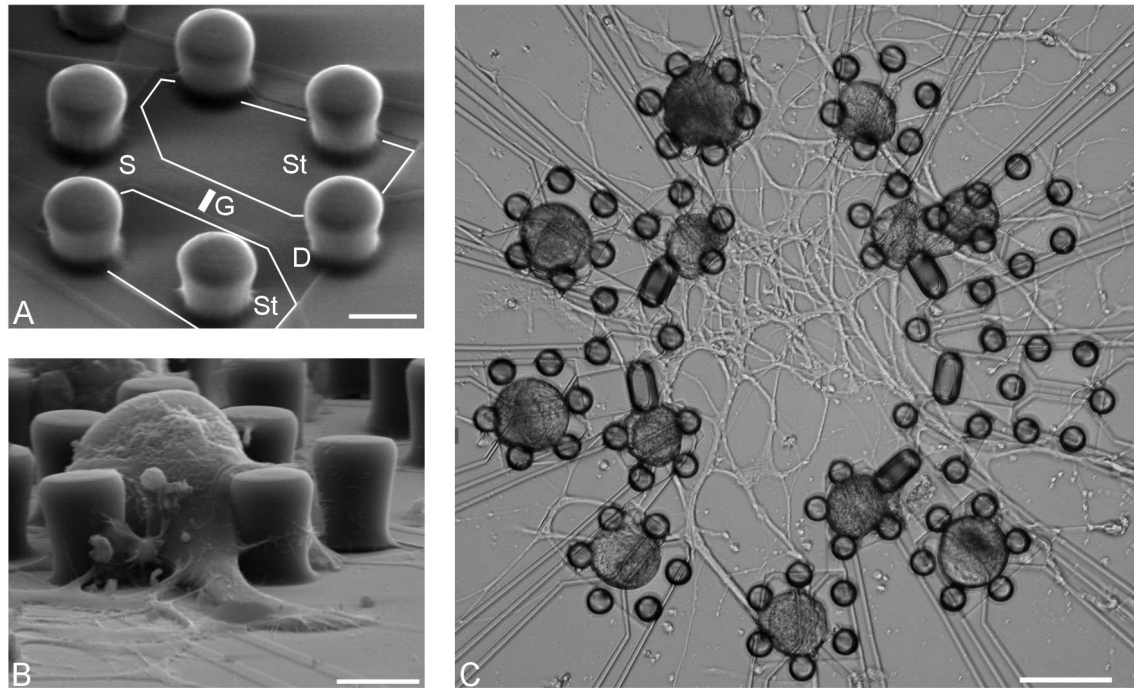
Zeck and Fromherz

Fig. 2. Neuron silicon chip. (*A*) Electronmicrograph of two-way contact with picket fence made of polyimide. Stimulator wings (St) and transistor (S, source; D, drain; G, gate) are marked. (Scale bar = 20 μm.) (*B*) Electronmicrograph, after fixation, of neuron from the A cluster of the pedal ganglia in *L. stagnalis* in a picket fence after 3 days in culture. (Scale bar = 20 μm.) (*C*) Micrograph of neuronal cell bodies (dark blobs) in picket fences on a circle of two-way contacts connected by neurites (bright threads) after 2 days in culture. The fences consist of six pickets in an outer ring and of five pickets in an inner ring where two pickets of adjacent fences are fused to bar-like structures. (Scale bar = 100 μm.)

cell membrane was recorded with a photomultiplier (R928, Hamamatsu Photonics, Hamamatsu City, Japan) using a lock-in amplifier. The sheet resistance r_J of the gap between chip and cell was obtained from a fit of the phase map with the theory of a planar core-coat conductor (ref. 27; D. Braun and P.F., unpublished results).

Electrophysiology. Neurons were impaled with glass microelectrodes (no. 1403547, Hilgenberg, Malsfeld, Germany) which were prepared with a multipurpose puller (Zeitz, Augsburg, Germany), filled with 4 M potassium acetate (resistance 15–25 MΩ), and contacted with Ag/AgCl electrodes. They were mounted on micromanipulators (Narishige, Tokyo) and connected to bridge-amplifiers (NPI Instruments, Tamm, Germany). The input conductances of the neurons and the strength of the electrical synapses were measured, applying hyperpolarizing currents of 0.3 nA. Action potentials were elicited by depolarizing currents of 0.3 nA for 30–60 ms.

Stimulation and Recording by the Chip. Bulk silicon was kept at +6.5 V with respect to the bath held on ground potential with a Ag/AgCl electrode. We kept the stimulator areas on ground potential and superposed bursts of positive stimulation pulses by using a waveform generator (33120A, Hewlett–Packard) under general purpose interface bus (GPIB) control. Width and separation of the rectangular pulses were 0.5 ms. The maximum pulse amplitude was +5 V to avoid electrical breakthrough of the oxide. We applied a bias of +1.5 V to the source and +0.5 V to the drain of the field effect transistor. The total source-drain current at the working point was $I_{SD} = 100$–150 μA. A change of the voltage on the gate of +10 mV induced a current modulation of -1 μA as checked before each measurement. The transients of the stimulators, of the impaled microelectrodes, and of the transistors were recorded by using a program written in LABVIEW (National Instruments, Austin, TX; ref. 19). The

sampling rate was adjusted to a constant number of 3000 samples per sweep. The stimulation peaks produced artifacts that differed between channels because of multiplexing of the analog-to-digital conversion and were too short to be recorded appropriately.

Results and Discussion

Outgrowth. A picket fence around a two-way contact of the chip is shown in Fig. 2*A*. Individual neurons from the A-cluster of the pedal ganglia of *L. stagnalis* were placed into the cages. Within two days, neurites sprouted without displacing the cell bodies from the contacts (Fig. 2*B*). A web of interacting neurites formed in the central area of the chip as illustrated in Fig. 2*C*. The mechanical fixation of the cell bodies with the open fences avoided problems with hindered nutrition and outgrowth, and with forces that lift the cells from the contact as they occur when fixation is attempted by pits in a substrate (28).

Neuron–Silicon Junctions. We investigated the structure of the neuron-silicon contact by FLIC microscopy on a silicon chip with four shallow terraces of silicon dioxide after staining the membrane with the cyanine dye DiIC$_{18}$ (24, 25). Fitting the experimental fluorescence intensities on the four terraces with the electromagnetic FLIC theory, we obtained a distance $d_J = 50 \pm 5$ nm ($n = 7$) between the attached cell membrane and the silicon dioxide. The area of cell adhesion was typically around $A_{JM} = 2000$ μm^2, which corresponded roughly to a fraction of 0.25 of the total cell surface.

The resistance of the gap between neuron and chip was obtained from the response of the cell membrane to AC stimulation from the chip after staining with the hemicyanine dye Annine 5 (R. Gleixner and P.F., unpublished results). By fitting a phase map of the fluorescence intensity with the theory of a planar core-coat conductor, a sheet resistance $r_J = 25 \pm 5$ MΩ ($n = 5$) was obtained. From the relation $r_J = \rho_J/d_J$, we
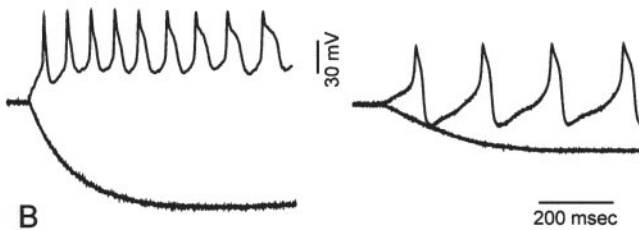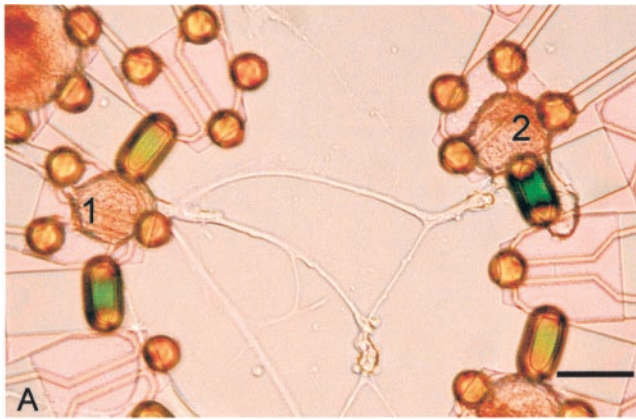
Fig. 3. Synaptically connected neuron pair from the A cluster of the pedal ganglia in *L. stagnalis* on silicon chip. (*A*) Neuron pair with cell bodies (dark blobs) in picket fences on two-way junctions. Neurites (bright threads) are grown from both cell bodies and meet at several places. Scale bar = 50 μm. Both neurons were impaled by micropipettes to check the intracellular voltage. (*B*) Intracellular voltage of neuron 1 and neuron 2 on hyperpolarizing (-0.3 nA) and depolarizing (0.3 nA) current injection in neuron 1.

estimated a specific resistance in the junction $\rho_J = 125$ $\Omega \cdot$cm, which was similar to the resistance of the bath. By using the relation $R_J = r_J/5\pi$ (27), we obtained a global resistance of the junction $R_J \approx 1.7$ MΩ. The specific conductance of the junction area $g_J = (R_J A_{JM})^{-1}$ was $g_J \approx 30$ mS/cm^2.

Electrical Synapses. Before studying electronic interfacing, we tested a neuron pair for electrical synapses. An example is shown in Fig. 3*A* where the two neurons were 250 μm apart on the chip and joined by several pathways of grown neurites. The position of synaptic contacts was unknown. When the cells were impaled with microelectrodes and a hyperpolarizing current was injected in neuron 1, we recorded a hyperpolarization in both cells (Fig. 3*B*). The ratio of the stationary post- and presynaptic hyperpolarization—the coupling coefficient—was $k_{SYN} = 0.45$. From the relation $k_{SYN} = G_{SYN}/(G_{SYN} + G_{POST})$, with G_{POST} the input conductance of the postsynaptic neuron (29), we obtained a synaptic conductance $G_{SYN} = 2$ nS. Similar results were observed for all other neuron pairs that were pre- and postsynaptically interfaced; the synaptic coupling coefficient was $k_{SYN} = 0.25 \pm 0.15$ ($n = 11$) and the synaptic conductance $G_{SYN} = 1.3 \pm 0.8$ nS.

When we applied a depolarizing current we observed a burst of action potentials (AP) in the presynaptic neuron (Fig. 3*B*). A burst of APs appeared in the postsynaptic neuron, too, although at a lower frequency. A summation of the postsynaptic effect of two to three presynaptic APs was required to elicit a postsynaptic AP. During an AP with an amplitude of 50 mV and a width of 50 ms, a charge of about 5 picocoulombs is transferred through an electrical synapse with conductance $G_{SYN} = 2$ nS. That postsynaptic stimulus corresponds to a current of 0.3 nA

for 16 ms, which was below the threshold to elicit an AP by a micropipette.

Interfaced Monosynaptic Loops. We applied a burst of voltage pulses (5 V height, 0.5 ms width, 0.5 ms separation) to the capacitive stimulator beneath one neuron and observed the response of the transistors beneath both neurons as well as both intracellular voltages via impaled micropipettes. The records for the neurochip shown in Fig. 3*A* are displayed in Fig. 4*A*. A burst of seven pulses was applied to excite neuron 1. The AP was recorded by the transistor underneath neuron 1. In neuron 2, we observed a subthreshold postsynaptic depolarization that was not detected by the transistor there. A second burst of voltage pulses elicited another AP in neuron 1 and led to a further subthreshold depolarization of neuron 2. After the third burst, which failed to stimulate neuron 1, the fourth burst gave rise to an AP in neuron 1 that finally induced a postsynaptic excitation in neuron 2. That postsynaptic AP was recorded by the transistor underneath neuron 2, completing the electronically interfaced monosynaptic loop. The temporal summation of postsynaptic potentials after capacitive stimulation of the presynaptic neuron corresponded to summation observed with intracellular stimulation of the presynaptic neuron (Fig. 3*B*).

We repeated the experiment 45 min later (Fig. 4B). A burst of 11 pulses was applied to elicit an AP in neuron 1, which led to a subthreshold depolarization in neuron 2. A second burst gave rise to a further AP in neuron 1, which induced a postsynaptic AP that was recorded by the transistor, demonstrating that the electronically interfaced monosynaptic loop existed for an extended time interval. In that experiment, the records of transistor 1 had a lower amplitude and those of transistor 2 a different shape, as compared with the previous records.

Correlated with the burst of stimulation pulses, we observed perturbations of both transistor records and of both microelectrode signals (Fig. 4 *A* and *B*). These perturbations did not reflect actual changes of the voltage on the gate or of the intracellular voltage, respectively. Control experiments without neurons revealed a direct pathway of capacitive coupling through the chip from stimulators to transistors. Control experiments with an open stimulator and a neuron far away revealed capacitive coupling to the micropipette through the bath. A slow subsequent depolarization of the cell was not observed in that case. On the other hand, the shape, the delay, and the temporal summation of the postsynaptic signals seen in Fig. 4 *A* and *B* corresponded to the experiment with intracellular presynaptic stimulation (Fig. 3*B*). Thus, we conclude that the depolarization of the postsynaptic neuron (Fig. 4) was induced by synaptic transmission and not by direct chip stimulation.

Statistics. We observed eleven monosynaptic loops that were interfaced by the chip and checked by intracellular recording similar to the experiment shown in Fig. 4. To elicit a presynaptic AP, the number of voltage pulses in a burst varied from 1 to 20. The efficiency of capacitive stimulation correlated with the alignment of the cell bodies on the stimulator area. The number of presynaptic APs required to yield a postsynaptic AP by temporal summation varied from one to four without correlation to the synaptic strength, presumably because of varying thresholds of the postsynaptic neuron. The pre- and postsynaptic transistor records had an amplitude of 0.3–2 mV with a variable shape. On the presynaptic side, the response was always positive, in phase with the AP or delayed by a few milliseconds. On the postsynaptic side, we observed seven positive, two negative, and two changing responses (*cf.* Fig. 4). All theses signals were delayed with respect to the APs.

Capacitive Stimulation. A changing voltage dV_s/dt applied to a stimulator gives rise to currents through oxide, membrane, and
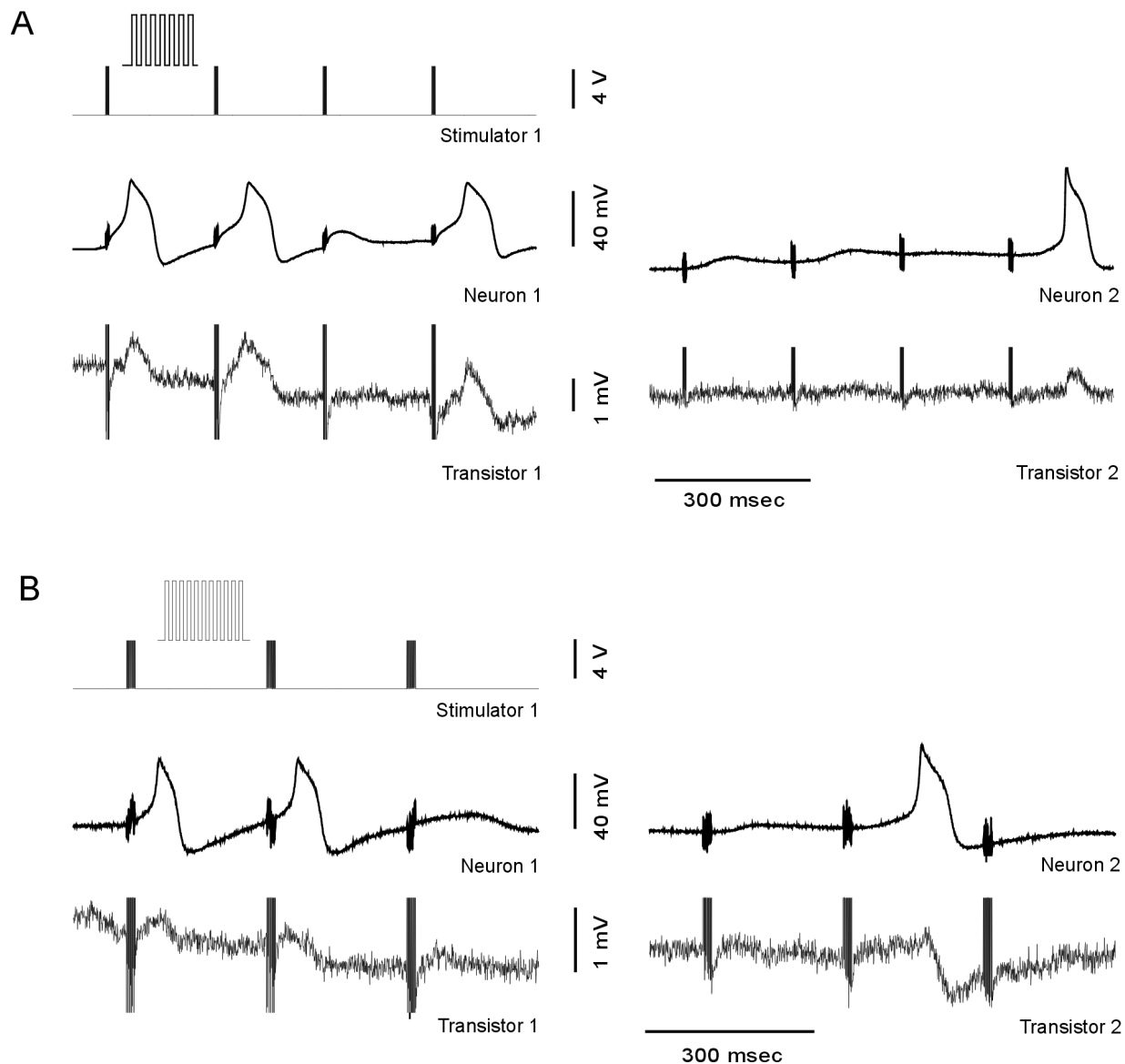
10460 | www.pnas.org/cgi/doi/10.1073/pnas.181348698

Zeck and Fromherz

Downloaded at Palestinian Territory, occupied on December 20, 2021

www.manaraa.com

Fig. 4. Neuroelectronic signal transmission. (*A*) First experiment. (*B*) Second experiment 45 min later. (*Left*) Neuron 1. From *Top* to *Bottom*: bursts of voltage pulses at the stimulator, intracellular voltage, and extracellular voltage on the transistor. (*Right*) Neuron 2. From *Top* to *Bottom*: intracellular voltage in neuron 2, extracellular voltage on the transistor. The *Insets* illustrate the stimulation pulses (amplitude 5 V, duration 0.5 ms) with bursts of 6.5 ms (7 pulses) in *A* and of 10.5 ms (11 pulses) in *B*, respectively. The perturbations of the intracellular and extracellular records that are correlated with the stimulation bursts do not reflect actual changes of intra- and extracellular voltage but are caused by capacitive coupling, through bath and chip from the stimulators to the micropipettes and to the transistors, respectively.

gap with capacitances $c_{OX} = 0.34$ μF/cm^2 and $c_M = 4$ μF/cm^2 and the conductance $g_J = 30$ mS/cm^2, respectively (Fig. 1*C*). The resulting extracellular voltage V_J may affect voltage-gated ion channels. Two elementary stimuli may be distinguished: (*i*) A voltage step of height V_S^{max}, which leads to an exponential extracellular transient $V_J \approx V_S^{max}(c_{OX}/c_M) \cdot \exp(-tg_J/c_M)$; and (*ii*) a ramp up to a height V_S^{max}, which leads to an extracellular voltage pulse with an amplitude $V_J \approx (c_{OX}/g_J)dV_S/dt$ and a width $\Delta t_J = V_S^{max}/(dV_S/dt)$. When we restrict the applied voltage to $|V_S^{max}| = 5V$ to avoid a breakthrough of the oxide, amplitude and time constant of the exponential are about 400 mV and 0.13 ms, and the width of the extracellular pulse is about 3 ms at an amplitude of 20 mV, respectively. Such individual stimuli were rarely able to elicit action potentials in snail neurons. We found, however, that repetitive application of voltage pulses of various shapes was always successful when applied sufficiently long.

Bursts of rectangular pulses were most effective. The mechanism of this AC stimulation is not clear. It may be related with the asymmetry in opening and closing rate constants of voltage-gated ion channels (M. Ulbrich and P.F., unpublished results).

Transistor Records. A firing neuron gives rise to ionic and capacitive currents through the attached membrane that flow along the gap above the transistor (Fig. 1*C*). A net current appears only if the cell membrane is electrically inhomogeneous. The resulting voltage change V_J on the gate can be expressed by the difference of the specific ion conductances g_{JM}^i and g_{FM}^i in the attached and free membrane and the specific conductance g_J of the junction according to $V_J(t) \approx g_J^{-1}\Sigma(g_{JM}^i - g_{FM}^i)(V_M - V_0^i)$, with the reversal voltages V_0^i (30). On this basis, we assign the low amplitudes of the transistor records (Fig. 4) to a rather homogeneous distribution of all ion

Zeck and Fromherz

conductances on the neuronal cell body with $(g_{JM}^i - g_{FM}^i) \ll g_J = 30$ mS/cm^2. The shape of the presynaptic transistor records resembled in many cases the intracellular APs (Fig. 4). That similarity indicates that a small Ohmic leak conductance in the attached membrane with $g_{JM} > g_{FM}$ played a role. The leaks may have been induced by the capacitive stimuli (10). The shapes of the postsynaptic records differed significantly from the intracellular voltages: e.g., the positive signal in Fig. 4A was delayed distinctly with respect to the AP, and the record in Fig. 4B had a trough in the late part of the AP. The delays suggest a role of potassium channels. With $V_M - V_0^K > 0$, a positive signal would indicate an enhanced conduction in the junction $g_{JM}^K > g_{FM}^K$, a negative amplitude a reduced conduction $g_{JM}^K < g_{FM}^K$. Such an enhancement and reduction of potassium conductances in cell-chip junctions was shown to exist with rat neurons (31).

Conclusion

We implemented and characterized the complete signaling pathway from a semiconductor chip through a circuit of nerve cells back to the semiconductor. The experiment constitutes a fundamental step in neuroelectronic engineering, in its combination of culturing neurons on an inert surface above a micro-electronically active substrate, immobilizing individual neurons on the contact sites without disruption by migration, and non-invasive electronic interfacing for stimulation and recording without impalement by micropipettes. The method is suitable for long-term studies on synaptic modulation in small networks of invertebrate neurons that are connected by chemical synapses.

To achieve electronically supervised nerve cell circuits as sketched in Fig. 1A, further progress is required in chip technology, bioelectronic interfacing, and neuronal growth techniques. Crucial aspects are (*i*) the fabrication of stimulators with higher capacitance and transistors with lower noise, (*ii*) the design of optimized neuronal contacts by transfection with ion channels (32), (*iii*) the control of the neuronal circuit by guided growth with defined synaptic junctions (18, 33), and (*iv*) the application of VLSI (very large scale integration) technology for chips with a large number of contact sites.

1. Mahowald, M. & Douglas, R. (1991) *Nature (London)* **354,** 515–518.
2. Sharp, A. A., Abbott, L. F. & Marder, E. (1992) *J. Neurophysiol.* **67,** 1691–1694.
3. Hopfield, J. J. (1982) *Proc. Natl. Acad. Soc. USA* **79,** 2554–2558.
4. Gross, G.W., Rieske, E., Kreutzberg, W. & Meyer, A. (1977) *Neurosci. Lett.* **6,** 101–105.
5. Pine, J. (1980) *J. Neurosci. Methods* **2,** 19–31.
6. Novak, J. L. & Wheeler, B. C. (1986) *IEEE Trans. Biomed. Eng.* **33,** 196–202.
7. Fromherz, P., Offenhäusser, A., Vetter, T. &. Weis, J. (1991) *Science* **252,** 1290–1293.
8. Fromherz, P. & Stett, A. (1995) *Phys. Rev. Lett.* **75,** 1670–1673.
9. Stett, A., Müller, B. & Fromherz, P. (1997) *Phys. Rev. E* **55,** 1779–1782.
10. Ulbrich, M. & Fromherz, P. (2001) *Adv. Mater.* **13,** 344–347.
11. Wolf, S. & Tauber, R. N. (1986) *Silicon Processing for VLSI Era* (Lattice Press, Sunset Beach, CA).
12. Rayport, S. G. & Schacher, S. (1986) *J. Neurosci.* **6,** 759–763.
13. Kleinfeld, D., Raccuia-Behling, F. & Chiel, H. J. (1990) *Biophys. J.* **57,** 697–715.
14. Syed, N. I., Bulloch, A. G. M. & Lukowiak, K. (1990) *Science* **250,** 282–285.
15. Kyriakides, M., McCrohan, C. R., Slade, C. T., Syed, N. I. & Winlow, W. (1989) *Comp. Biochem. Physiol.* **93,** 861–876.
16. Ridgway, R. L., Syed, N. I., Lukowiak, K. & Bulloch, A. G. M. (1991) *J. Neurobiol.* **22,** 377–390.
17. Hadley, R. D., Kater, S. B. & Cohan, C. S. (1983) *Science* **221,** 466–468.
18. Prinz, A. A. & Fromherz, P. (2000) *Biol. Cybern.* **82,** L1–L5.
19. Jenkner, M., Müller, B. & Fromherz, P. (2001) *Biol. Cybern.* **84,** 239–249.
20. Kiessling, V., Müller, B. & Fromherz, P. (2000) *Langmuir* **16,** 3517–3521.
21. Rentschler, M. & Fromherz, P. (1998) *Langmuir* **14,** 547–551.
22. Wong, R. G., Hadley, R. D., Kater, S. B. & Hauser, G. C. (1981) *J. Neurosci.* **1,** 1008–1021.
23. Wong, R. G., Martel, E. C. & Kater, S. B. (1983) *J. Exp. Biol.* **105,** 389–393.
24. Lambacher, A. & Fromherz, P. (1996) *Appl. Phys. A* **63,** 207–216.
25. Braun, D. & Fromherz, P. (1997) *Appl. Phys. A* **65,** 341–348.
26. Braun, D. & Fromherz, P. (2001) *Phys. Rev. Lett.* **86,** 2905–2908.
27. Weis, R. & Fromherz, P. (1997) *Phys. Rev. E* **55,** 877–889.
28. Maher, M. P., Pine, J., Wright, J. & Tai, Y. C. (1999) *J. Neurosci. Methods* **87,** 45–56.
29. Bodmer, R., Dagan, D. & Levitan, I. B. (1984) *J. Neurosci.* **4,** 228–233.
30. Fromherz, P. (1999) *Eur. Biophys. J.* **28,** 254–258.
31. Vassanelli, S. & Fromherz, P. (1999) *J. Neurosci.* **19,** 6767–6773.
32. Straub, B., Meyer, E. & Fromherz, P. (2001) *Nat. Biotech.* **19,** 121–124.
33. Fromherz, P. & Schaden, H. (1994) *Eur. J. Neurosci.* **6,** 1500–1504.